

**¹ A mechanistic model (BCC-PSSICO) to predict
² changes in the hydraulic properties for bio-amended
³ variably saturated soils**

Albert Carles Brangarí,^{1,2} Xavier Sanchez-Vila,^{1,2} Anna Freixa,³ Anna M.

Romani,³ Simonetta Rubol,⁴ and Daniel Fernàndez-Garcia^{1,2}

Corresponding author: Albert C. Brangarí, Department of Civil and Environmental Engineering, Universitat Politècnica de Catalunya (UPC), Jordi Girona 1-3, 08034 Barcelona, Spain (albert.carles@upc.edu)

¹Department of Civil and Environmental

Key Points.

- A new mechanistically-based model to estimate the impact of complex biofilms on the soil hydraulic properties.
- We derive a set of analytical equations for water retention and relative permeability.
- The model is corroborated by using real data from laboratory experiments and previously existing models.

4 **Abstract.** The accumulation of biofilms in porous media is likely to in-
5 fluence the overall hydraulic properties and, consequently, a sound under-
6 standing of the process is required for the proper design and management

Engineering, Universitat Politècnica de
Catalunya (UPC), Jordi Girona 1-3, 08034
Barcelona, Spain.

²Associated Unit: Hydrogeology Group
(UPC-CSIC).

³Institute of Aquatic Ecology,
Department of Environmental Sciences,
University of Girona, Campus Montilivi
17071 Girona, Spain.

⁴Department of Biological Sciences,
Marine Environmental Biology Section,
University of Southern California, Los
Angeles, CA 90089, USA.

7 of many technological applications. In order to bring some light into this phe-
8 nomenon we present a mechanistic model to study the variably saturated hy-
9 draulic properties of bio-amended soils. Special emphasis is laid on the dis-
10 tribution of phases at pore-scale and the mechanisms to retain and let wa-
11 ter flow through, providing valuable insights into phenomena behind bioclog-
12 ging. Our approach consists in modeling the porous media as an ensemble
13 of capillary tubes, obtained from the biofilm-free water retention curve. This
14 methodology is extended by the incorporation of a biofilm composed of bac-
15 terial cells and extracellular polymeric substances (EPS). Moreover, such a
16 microbial consortium displays a channeled geometry that shrinks/swells with
17 suction. Analytical equations for the volumetric water content and the rel-
18 ative permeability can then be derived by assuming that biomass reshapes
19 the pore space following specific geometrical patterns. The model is discussed
20 by using data from laboratory studies and other approaches already exist-
21 ing in the literature. It can reproduce i) displacements of the retention curve
22 towards higher saturations and ii) permeability reductions of distinct orders
23 of magnitude. Our findings also illustrate how even very small amounts of
24 biofilm may lead to significant changes in the hydraulic properties. We there-
25 fore state the importance of accounting for the hydraulic characteristics of
26 biofilms and for a complex/more realistic geometry of colonies at the pore-
27 scale.

1. Introduction

28 The vadose zone is of major interest because of its role in the environment and in
29 human life [*Selker et al.*, 1999]. The reason why the unsaturated zone is so appealing is
30 that it connects different environmental compartments providing water and nutrients to
31 the biosphere. As a result of this interaction, a wide range of bio-mediated processes with
32 potential to modify soil characteristics are triggered [*DeJong et al.*, 2013].

33 In the middle of the twentieth century, engineers and soil scientists started paying at-
34 tention to the significance of bio-mediated soil processes for the design and management
35 of technological applications. One example where bioclogging has strong implications is
36 the infiltration of water in recharge facilities, characterized by a pro-con dichotomy. On
37 the one hand, the accumulation of biomass might be considered a disadvantage because
38 it partially blocks flow paths [*Engesgaard et al.*, 2006; *Seki et al.*, 1998; *Vandevivere and*
39 *Baveye*, 1992a; *Yarwood et al.*, 2006; *Zhong and Wu*, 2013], diminishing the efficiency of
40 recharge ponds [*Baveye et al.*, 1998; *Pedretti et al.*, 2012], drainage fields [*Kennedy and*
41 *Van Geel*, 2001], wetlands [*Morris et al.*, 2011; *Samsó and García*, 2014], and biofilters
42 [*Mauclaire et al.*, 2006; *Soleimani et al.*, 2009]. On the other hand, the presence of bacte-
43 rial communities has proved beneficial, as for example, it increases water retention time
44 [*Van Cuyk et al.*, 2001], eventually facilitating the removal of contaminants [*Christensen*
45 *et al.*, 2000; *Rodríguez-Escales et al.*, 2016; *Zhang et al.*, 1995]. Moreover, biomass driven
46 permeability reduction may be exploited in geotechnical engineering [*Castegnier et al.*,
47 2006; *Ross et al.*, 2001], in CO_2 sequestration [*Cunningham et al.*, 2009], and in oil recov-

48 ery [*Abdel-Waly*, 2013]. Therefore, whether biomass accumulation proves to be an overall
49 advantage or a drawback depends on the particular circumstances.

50 The largest and most diverse bacterial population in the biosphere coexists in the vadose
51 zone [*Or et al.*, 2007a]. Many studies have pointed out the existence of large amounts
52 of bacteria forming aggregates of cells [e.g., *De Beer and Schramm*, 1999; *Vandevivere*
53 *and Baveye*, 1992a]. Most bacteria are embedded, to a greater or lesser extent, in a self-
54 produced matrix forming biofilms attached to soil particles [*Fenchel*, 2002; *Young and*
55 *Crawford*, 2004]. Such a matrix is composed of a combination of solids [*De Muynck et al.*,
56 2010; *Ehrlich*, 1999], gaseous by-products [*Rebata-Landa and Santamarina*, 2012; *Seki*
57 *et al.*, 1998], and extracellular polymeric substances (EPS) [*Flemming and Wingender*,
58 2010; *Stoodley et al.*, 2002]. Moreover, biofilm comprises complex structures of intricate
59 strandlike architecture that forms pores, voids and channels [*Stewart*, 2012; *Stoodley et al.*,
60 1994; *Wagner et al.*, 2010].

61 The accumulation of such a complex biomass in soils alters the pore geometry, and it
62 is known to trigger significant changes in the hydraulic properties [*Bozorg et al.*, 2015;
63 *Rockhold et al.*, 2002; *Or et al.*, 2007a]. However, it is difficult to correlate a given biofilm
64 colonization with such changes. The capacity of microbial communities to dynamically
65 adapt to the environmental conditions [*Kim et al.*, 2010; *Wilking et al.*, 2011] hampers
66 the formulation of general models. This highlights the need for a sound understanding of
67 the components and structure of the microbial community, as well as of their spatial dis-
68 tribution. A number of strategies with varying degrees of complexity have been adopted
69 to evaluate the effects of biomass accumulation on the hydraulic properties. Some stud-
70 ies treat biofilm from a macroscopic point of view without assuming a specific pattern.

71 *Clement et al.* [1996] defined analytical expressions to account for porosity and permeabil-
72 ity changes in saturated porous media. *Rockhold et al.* [2002] presented a composite media
73 model in which these definitions were extended to unsaturated soils. *Rosenzweig et al.*
74 [2012] explored the effect of EPS on the soil-water retention curve (SWRC) by using sim-
75 ple superposition. In contrast, some studies aim at describing biofilm and porous media in
76 detail. Early studies modeled biofilm in saturated media as a continuous layer of uniform
77 thickness covering the soil grains [*Rittmann, 1993; Taylor et al., 1990; Cunningham et al.,*
78 1991] or as discrete microcolonies [*Vandevivere and Baveye, 1992a*]. *Mostafa and Van Geel*
79 [2007, 2012] incorporated the presence of EPS and the distinction between active and inert
80 biomass into the impermeable biofilm model. The permeability formulations were based
81 on the approaches proposed by *Burdine* [1953] and *Mualem* [1976]. Meanwhile, *Thullner*
82 *and Baveye* [2008] studied the use of biofilm layers embedded in cylindrical pores, and
83 found that permeable biofilms growing in pore-networks are capable of simulating per-
84 meability reductions similar to the ones found in literature. Later on, *Rosenzweig* and
85 coworkers focused on the effects of the distribution of impermeable biomass in unsatu-
86 rated conditions. They assumed that biofilms cover the walls of cylindrical capillary tubes
87 [*Rosenzweig et al., 2009*] or of a pore-network consisting of triangular channels [*Rosen-*
88 *zweig et al., 2013, 2014*]. Similarly, *Ezeuko et al.* [2011] and *Qin and Hassanizadeh* [2015]
89 used geometries of increased complexity.

90 The present study provides a new mechanistic model that simulates the changes in the
91 SWRC and the relative permeability induced by biofilm accumulation. Soil is represented
92 as an ensemble of capillary tubes colonized by a complex biofilm. It is well known that
93 this interpretation does not consider dual-occupancy or connectivity [*Likos and Jaafar,*

2013; *Beckett and Augarde*, 2013]; nevertheless, its use is quite standard in soil hydraulics
[e.g., *Thullner and Baveye*, 2008; *Mostafa and Van Geel*, 2007; *Rosenzweig et al.*, 2009].
For the sake of simplicity it is used here as a first step towards a more realistic representation of biofilm complexity. The microbial phase in this model has six elements that are synthesized in the acronym PSSICO. Letter “P” stands for Porous, which indicates that the biomass matrix has an internal secondary porosity. “S” denotes Sticking, as we model only the biomass that grows attached to the solids, and not the one remaining in suspension. The second “S” implies that the microbial phase has Swelling properties, which changes volume and rheological properties in response to suction by absorbing/exuding water. “I” stands for Identifiable, denoting that the model requires a quantification of biomass from laboratory or field data, or estimated from a model. “C” is referred to the potential presence of biofilm Channels through which water can easily flow or be retained. Finally, “O” indicates that the biofilm is treated as a separate Object in a composite medium.

Using PSSICO, we developed a flexible theoretical model in an attempt to elucidate the mechanisms conditioning water retention and flow through bio-amended systems. Distinguishing between water in biofilms and in the pore-matrix, a set of analytical equations for saturation and relative permeability is derived. The model is used then to simulate the changes in the SWRC observed in two laboratory experiments. The results obtained are discussed and compared to other biofilm models from the literature. Finally, some conclusions are drawn from the sensitivity analysis of the parameters.

2. Conceptual Model

2.1. Water in Bio-amended Soils

115 Based on *Rockhold et al.* [2002], *Rosenzweig et al.* [2012], and *Taylor et al.* [1990], the
 116 accumulation of biomass leads to an increase in soil moisture for several reasons: i) the
 117 size and shape of the pore-matrix is altered by the accumulation of products, generating
 118 changes in the structure and connectivity of soils; ii) the biofilm contains a liquid phase
 119 mostly constituted by water; and iii) the wettability patterns of soils surfaces are modified.
 120 The total water content in bio-amended soils (θ_{tot}) may be defined as the sum of the
 121 volume associated with the microbial phase ($\theta_{w,bio} + \theta_{r,bio}$) and that of the pore-matrix
 122 ($\theta_{w,pm} + \theta_{r,pm}$),

$$\theta_{tot} = \theta_{w,bio} + \theta_{w,pm} + \theta_{r,bio} + \theta_{r,pm} = \theta_w + \theta_r, \quad (1)$$

123 where the subscripts r and w respectively determine whether water is in the residual state
 124 (irreducible) or not. The maximum value of θ_{tot} in (1) is equal to the porosity of the soil.
 125 Thus, when biofilm occupies the pore space it is at the expense of the portion initially
 126 available for open-pore water. The presence of biofilm components other than water
 127 (mainly solids particles), which would prevent the occurrence of full water saturation is
 128 neglected (details below).

2.2. Water in Biofilms

129 The complex structure and composition of biofilms [see *Flemming and Wingender*, 2010;
 130 *Or et al.*, 2007b; *Piciooreanu et al.*, 2004] demands the use of a multifaceted definition of
 131 the microbial phase, which is achieved from the *six* elements of PSSICO. First, a proper
 132 Identification of the microbial phase is needed (component “I” in the model). Second,
 133 the treatment of the microbial phase in the literature has several interpretations. Some

134 authors treat it as a single unit [e.g., *Soleimani et al.*, 2009], whereas others stress the
 135 need to distinguish even between five types of microbial products [e.g., *Laspidou and*
 136 *Rittmann*, 2004]. In this paper we focus on the sticking (“S”) biomass attached to soil
 137 grains, regardless of its origin (growth, reattachment, trapping or others). We disregard
 138 the biomass in suspension and soluble products that are less likely to modify hydraulic
 139 properties. Thus, biofilm consists of bacteria and EPS so that

$$M_{bio}(t) = M_{bact}(t) + M_{EPS}(t), \quad (2)$$

140 where M_{bact} , M_{EPS} , and M_{bio} are respectively the masses of bacteria, EPS, and total
 141 biofilm, expressed in grams of dry mass per unit volume. The time variable (t) denotes
 142 that biofilm composition may change with time.

143 Concerning its structure, biofilms can be seen as a complex three-dimensional network
 144 of strands of EPS and bacteria forming voids and channels (Figure 1). Such structure has
 145 significant implications in the way biofilm interacts with water; actually it behaves like a
 146 sponge with a large absorbing capacity that shrinks/swells with suction changes ([*Or et al.*,
 147 2007b]). Under favorable hydration conditions, the EPS shows an open structure that can
 148 hold up to 70 times its weight in water [*Chenu*, 1993]. On the contrary, biofilms respond
 149 by shrinking when suction increases becoming dense and amorphous, albeit holding a
 150 considerable amount of water. Such a mechanism enhances dehydration resistance and
 151 fast recovery swelling after desiccation [*Tamaru et al.*, 2005], minimizing the impact of
 152 dry conditions upon bacterial life [*Or et al.*, 2007b].

153 According to *de Gennes* [1979], the equilibrium mass ratio between a polymer and water
 154 may be defined by a power-law of suction; assuming further that only the EPS behaves

155 like a polymer, the volume of mobile water in biofilms is estimated by

$$\theta_{w,bio}^*(\psi, M_{bio}) = \frac{M_{EPS}}{\rho_w} A \psi^{-B}, \quad (3)$$

156 where ψ is the matric suction (in cm), ρ_w the density of water, and A , B are fitting
 157 experimental parameters. *Rosenzweig et al.* [2012] found values of $A = 105.76$ and $B =$
 158 0.489 for pure xanthan ($C_{35}H_{49}O_{29}$), a natural polysaccharide widely used as an EPS
 159 analog [*Chenu, 1993; Rosenzweig et al., 2012*]. Nevertheless, the hydraulic properties
 160 of EPS depend on its specific composition. Particularly, xanthan depicts an outstanding
 161 retention capacity that is larger than other polysaccharides such as scleroglucan or dextran
 162 [*Chenu, 1993*]. Our model can effortlessly incorporate other type of relations (general or
 163 specific for a given study case) since it is not limited by working assumptions in (3-7).

164 The boundless behavior of $\theta_{w,bio}^*$ when ψ approaches zero demands the imposition of
 165 some restrictions in (3) that indirectly limits the volumetric density of biofilms. The
 166 maximum amount of water kept by biofilm is defined equal to 70 times its own mass
 167 [based on *Chenu, 1993*], and it is also limited by the effective porosity (ϕ_{ef}). Thus, we
 168 can rewrite the volume of water in biofilms in porous media applying such bounds as

$$\theta_{w,bio}(\psi, M_{bio}) = \min\left(\theta_{w,bio}^*, 70 \frac{M_{bio}}{\rho_w}, \phi_{ef}\right). \quad (4)$$

169 On the other hand, it seems logical to link $\theta_{r,bio}$ to the composition of the biofilm. From
 170 the contributions of bacterial cells and EPS we obtain

$$\theta_{r,bio}(M_{bio}) = 0.8 \frac{M_{bact}}{\rho_w} + \frac{M_{EPS}}{\rho_s} \theta_{r,EPS}, \quad (5)$$

171 where ρ_s is the bulk dry soil density and $\theta_{r,EPS}$ the residual water content for pure EPS.
 172 The first term in (5) considers the volume retained inside the body of bacteria. Water
 173 in cells is considered fully irreducible regardless of the environmental conditions, and it

174 is here quantified as 80% of the cellular volume [Cooke and Kuntz, 1974]. The remaining
 175 volume is neglected. The second term in (5) accounts for water in the polymeric matrix.
 176 The lack of information is overcome by assuming that under oven-dry suction the EPS
 177 can hold as much water as a clay material [inspired from Peña-Cabrales and Alexander,
 178 1979; Rockhold et al., 2002], $\theta_{r,EPS} \equiv \theta_{r,clay}$. Such a value is available in the literature
 179 [e.g., Carsel and Parrish, 1988], albeit it still displays high variability among studies.

2.3. Water Flow through Biofilms

180 Technological advances in instrumentation have demonstrated that water flows through
 181 biofilms [Billings et al., 2015]. Besides the intrinsic permeability of biological materials,
 182 void structures act as preferential flow paths that confer significant permeability to the
 183 biofilm [Davit et al., 2013; De Beer and Schramm, 1999; Lawrence et al., 1991]. There-
 184 fore, the flow capacity depends on both the structure and composition of the biofilm con-
 185 stituents. We simply assume here that the water flowing through biofilms has a dynamic
 186 viscosity (μ_{bio}) different from that in the pore-matrix (μ_w) [as in Qin and Hassanizadeh,
 187 2015; Pintelon et al., 2012; Thullner and Baveye, 2008]. This hypothesis, which was first
 188 proposed by Dupin et al. [2001], states that

$$\mu_{bio}(\psi) = \lambda_{\mu}(\psi)\mu_w, \quad (6)$$

189 where λ_{μ} (always greater or equal to 1) specifies the increased resistance of water flowing
 190 through biofilm. Since there are no specific studies on the effect of shrinking/swelling in
 191 λ_{μ} , we postulate the following expression

$$\lambda_{\mu} = \frac{1}{1 - \left[\frac{\theta_{r,bio}}{\theta_{w,bio} + \theta_{r,bio}} \right]^{\eta}}, \quad (7)$$

192 where η is a dimensionless parameter accounting for the stiffness of the viscous variation
 193 effect. The smaller the value of η , the more impermeable the biofilm. Figure 2 shows
 194 that when $\theta_{w,bio}$ is very high with respect to $\theta_{r,bio}$, the microbial phase is diluted and λ_μ
 195 tends to 1. When $\lambda_\mu = 1$ the water contained in biofilms flows as in the pore-matrix. In
 196 contrast, when biofilm shrinks and becomes denser, λ_μ increases tending to infinity.

3. The BCC-PSSICO Model

3.1. The Retention Curve of a Bio-amended Soil

197 Based on the capillary tube analogy, soil pores are replaced by a bundle of cylindrical
 198 capillaries (BCC) of different diameters. Let $f(r_0)$ be the frequency distribution of pore
 199 radii associated with a biofilm-free soil so that $f(r_0)dr_0$ is the number of capillary tubes
 200 per unit area with radii ranging between r_0 and $r_0 + dr_0$ before any biofilm is formed. We
 201 assume that the largest water-filled capillary tube available at a given matric suction ψ_0 ,
 202 denoted as R_0 , is obtained from the capillary rise equation

$$\psi_0 = \frac{2\sigma \cos(\beta)}{R_0 \gamma_w}, \quad (8)$$

203 where σ is the surface tension, β the contact angle and γ_w the specific weight of water.
 204 Then, the open-pore water content of a biofilm-free soil may be written as

$$\theta_{w,pm}^0(R_0) = \int_{R_{0,min}}^{R_0} \pi r_0^2 f(r_0) dr_0, \quad (9)$$

205 yielding

$$f(r_0) = \frac{2\sigma \cos(\beta)}{\gamma_w \pi r_0^4} \frac{d\theta_{w,pm}^0}{d\psi_0}, \quad (10)$$

206 where $R_{0,min}$ is the minimum pore radius. This value may be estimated from (8) using the
 207 maximum soil suction, which is generally considered in the order of 10^5 m [e.g., *Mitchell*
 208 *and Soga*, 2005]. The term $d\theta_{w,pm}^0/d\psi_0$ is the derivative of the SWRC expression. Despite

209 many alternatives can be used [e.g., *Brooks and Corey*, 1964], the van Genuchten equation
 210 (11) and its derivative (12) are simple, continuous and match the SWRC for a variety of
 211 soils by using only two fitting parameters (n and α) [*van Genuchten*, 1980].

$$\theta_{w,pm}^0(\psi_0) = \phi_{ef} \left[1 + [\alpha\psi_0]^n \right]^{\frac{1}{n}-1} \quad (11)$$

$$\frac{d\theta_{w,pm}^0(\psi_0)}{d\psi_0} = \alpha\phi_{ef}[1-n][\alpha\psi_0]^{n-1} \left[1 + [\alpha\psi_0]^n \right]^{\frac{1}{n}-2} \quad (12)$$

213 However the presence of biomass reshapes the open porosity with the result that the
 214 content of open-pore water becomes

$$\theta_{w,pm}(R) = \int_{R_{min}}^R \pi r^2 f(r) dr, \quad (13)$$

215 where $f(r)$ is the new pore-size distribution of the bio-amended soil. The matric suction
 216 at which the transformed tube radius empties is still given by the capillary rise equation,
 217 written now as

$$\psi = \frac{2\sigma \cos(\beta)}{R\gamma_w}. \quad (14)$$

218 Then, the relation between (8) and (14) may be expressed as

$$\psi = \frac{\psi_0}{X}, \quad (15)$$

219 where X is a parameter that will be defined and discussed below.

220 The spatial competition between open-pore water and biofilm is illustrated in Figure
 221 3. Note that when $\psi = \psi_{max}$, the volume of water in the biofilm is minimum (residual)
 222 and $\theta_{w,bio} = 0$; but it rises as suction decreases, modifying the open porosity. The char-
 223 acteristics of the new pores depend on how biomass reshapes the capillary tubes. Some
 224 previous studies consider that biofilm forms a layer attached to the pore walls [e.g. *Ezeuko*
 225 *et al.*, 2011; *Mostafa and Van Geel*, 2007; *Rosenzweig et al.*, 2009]. The distribution pat-
 226 terns of this biofilm depend on whether it grows preferentially either in the smaller or

227 in the larger pores, or uniformly in all of them [see the lucid discussions in *Bundt et al.*,
 228 2001; *Mostafa and Van Geel*, 2007; *Rosenzweig et al.*, 2009]. Although the distribution
 229 and morphology at the pore-scale is still an unresolved challenge, from the experimental
 230 evidence (see Figure 1) we consider that biofilms bring about changes in the pore-size
 231 distribution according to two mechanisms:

232 (i) the number of capillary tubes per unit soil area between r_0 and $r_0 + dr_0$ increases by
 233 a factor N so that

$$f(r)dr = Nf(r_0)dr_0, \quad (16)$$

234 (ii) the new tube radii are reduced by a positive real factor $X(\leq 1)$ with the result that

$$r = Xr_0. \quad (17)$$

235 Such a new combination of mechanisms allow the biofilm to show a relatively flexible
 236 architecture since it may be partially detached from the walls being located in the middle
 237 of the tubes cross-section. From a practical standpoint, this means that every single
 238 tube of radius r_0 is converted into N equal cylindrical tubes of radius r , reproducing
 239 structural channels embedded in the biofilm matrix. The effect of this transformation
 240 may be observed in Figure 4.

241 Substituting (16) and (17) into (13), we have

$$\theta_{w,pm}(R) = NX^2 \int_{R_{0,min}}^{R_0} \pi r_0^2 f(r_0) dr_0 = NX^2 \theta_{w,pm}^0(R_0), \quad (18)$$

242 where, from (15), the pore-matrix water content is

$$\theta_{w,pm}(\psi) = NX^2 \theta_{w,pm}^0(\psi_0) = NX^2 \theta_{w,pm}^0(X\psi), \quad (19)$$

243 and the retention curve for bio-amended soils may finally be written as

$$\theta_{tot}(\psi, M_{bio}) = \theta_{w,bio}(\psi, M_{bio}) + NX^2 \theta_{w,pm}^0(X\psi) + \theta_{r,bio}(M_{bio}) + \theta_{r,pm}. \quad (20)$$

244 Assuming that the effective porosity of the system has not changed or is known, the
 245 continuity equation

$$\phi_{ef} = \theta_{w,bio}(\psi, M_{bio}) + \theta_{w,pm}(\psi = 0) \quad (21)$$

246 must be fulfilled, the following relationship is therefore satisfied

$$NX^2 = 1 - \frac{\theta_{w,bio}(\psi, M_{bio})}{\phi_{ef}}, \quad (22)$$

247 and the tube-reduction factor X becomes

$$X(\psi, M_{bio}) = \sqrt{\frac{\phi_{ef} - \theta_{w,bio}(\psi, M_{bio})}{N\phi_{ef}}}. \quad (23)$$

248 Note that when both X and NX^2 approach 1 the impact of biofilm is negligible. However,
 249 as the values of $\theta_{w,bio}$ and/or N increase, the water retention curve in (20) differs more
 250 and more from that of the biofilm-free soil.

251 Several considerations about this model should be made. The existence of a constant X
 252 regardless of tube size means that biofilms proliferates in pores of all sizes. The amount of
 253 biomass in each tube is proportional to its squared radius and therefore the higher amounts
 254 of biomass are found in the larger tubes. These large tubes probably act as preferential
 255 paths through which nutrients may travel easily, promoting high growth rates. But at the
 256 same time, they also involve high velocities and high detachment effects [*Thullner and*
 257 *Baveye, 2008*], and are more likely to be exposed to drying periods [*Bundt et al., 2001*].
 258 Despite the flow limitations in smaller pores, growth is still expected because some nutri-
 259 ents can be available through diffusion. Moreover, the potential entrapping of suspended
 260 biomass on pore throats [*Vandevivere et al., 1995*] may lead to additional accumulation
 261 in small tubes. On the other hand, the use of the parameters N and M_{bio} may allow to
 262 better simulate the influence of the bioaccumulation since some mechanisms that were not

263 considered in previous models are now introduced. Using N , a complex biofilm structure
 264 not exclusively attached to the soil grains but lying in the middle of pores is described.
 265 It is worth noting that such an architecture is probably a product of the environmental
 266 conditions and that such conditions and therefore N are spatially heterogeneous and tem-
 267 porally variable. However, we considered it as a fitting parameter since further research
 268 is needed to relate N to measurable/estimable properties. Finally, despite M_{bio} can be
 269 measured more or less accurately, the quantification of its impact on pore space presents
 270 some difficulties, requiring the use of approaches or indirect estimations as the equations
 271 defined above.

3.2. Relative Permeability of Bio-amended Soils

272 Despite the simplifications inherent in the BCC-based models, we propose a simple for-
 273 mulation to examine the impact that a PSSICO biofilm has on the relative permeability
 274 curve. The hydraulic conductivity of a bio-amended soil is evaluated by combining the
 275 pore-size distribution with the HagenPoiseuille equation for laminar flow, which deter-
 276 mines that the flow rate in a tube (Q_{tube}) is proportional to the fourth power of its radius
 277 [Alaoui et al., 2011; Thullner and Baveye, 2008],

$$Q_{tube}(r) = \nabla h \frac{\gamma_w \pi}{8\mu_w} r^4, \quad (24)$$

278 where ∇h is the hydraulic head gradient. Following Thullner and Baveye [2008], when a
 279 biomass layer of thickness δ coats the tube walls (24) is transformed to

$$Q_{tube+bio}(r) = \nabla h \frac{\gamma_w \pi}{8\mu_{bio}} \left[[r + \delta]^4 - r^4 [1 - \lambda_\mu] \right]. \quad (25)$$

280 Nevertheless, the permeable biofilm coats all the tubes including those larger than R ,
 281 which are devoid of open-pore water according to (14). The total flow rate may be

282 obtained by limiting the flow contribution to the area between r and $r + \delta$ so that

$$Q_{bio}(r) = \nabla h \frac{\gamma_w \pi}{8\mu_{bio}} \left[[r + \delta]^4 + r^4 - 2r^2[r + \delta]^2 \right]. \quad (26)$$

283 It is worth noting that for values of $N > 1$ there is no symmetry around the central
284 axis of the tubes (recall Figure 4), ruling out the possibility of using (25,26) directly. To
285 overcome this problem we treat the entities separately (Figure 5). Since the areas are
286 preserved, it follows that

$$N\pi[r + \delta]^2 = \pi r_0^2, \quad (27)$$

287 being the relations between radii

$$r + \delta = \frac{r_0}{\sqrt{N}} = \frac{r}{X\sqrt{N}}. \quad (28)$$

288 The total flow rate in soil may be written as

$$\begin{aligned} q_{soil}(\psi) &= -K_s k_r \nabla h = \int_{R_{min}}^R Q_{tube+bio}(r) f(r) dr + \int_R^{R_{max}} Q_{bio}(r) f(r) dr \\ &= \int_{R_{0,min}}^{R_0} Q_{tube+bio}(Xr_0) N f(r_0) dr_0 + \int_{R_0}^{R_{0,max}} Q_{bio}(Xr_0) N f(r_0) dr_0, \end{aligned} \quad (29)$$

289 where K_s is the real saturated hydraulic conductivity and k_r the relative permeability.

290 Finally, substituting (25) and (26) into (29), we obtain

$$k_r(\psi) = \frac{\left[\frac{N^{-1} + N(\lambda_\mu - 1)X^4}{\lambda_\mu} \right] \int_{X\psi_{max}}^{X\psi} \frac{1}{\psi_0^2} \frac{d\theta_{w,pm}^0}{d\psi_0} d\psi_0 + \left[\frac{N^{-1} + (N - 2)X^4}{\lambda_\mu} \right] \int_{X\psi}^{X\psi_{min}} \frac{1}{\psi_0^2} \frac{d\theta_{w,pm}^0}{d\psi_0} d\psi_0}{\int_{\psi_{max}}^{\psi_{min}} \frac{1}{\psi_0^2} \frac{d\theta_{w,pm}^0}{d\psi_0} d\psi_0}, \quad (30)$$

291 which under saturated conditions or when $X = 0$ may be rewritten as

$$k_r(\psi) \equiv \frac{N^{-1} + N(\lambda_\mu - 1)X^4}{\lambda_\mu}. \quad (31)$$

292 Note that despite the fact that λ_μ and X are suction-dependent parameters, both can
293 be moved out of the integrals in (30) since the suction is constant in the equation.

4. Comparison with Experimental Data

294 The hypotheses assumed during the derivations were tested against two different data
295 sets reported in the literature. Table 2 lists the physical properties of water that were
296 used in the analysis.

297 In the first data set [Rosenzweig *et al.*, 2012] a sandy soil (Hamra) was artificially
298 mixed with xanthan. Theoretically, the use of such a methodology keeps the holding
299 characteristics of the EPS and avoids dealing with the presence of live bacteria. The mass
300 fractions in the xanthan-soil mixture were 0.25% and 1% in dry weight, equivalent to
301 $3.91 \cdot 10^{-3}$ and $1.576 \cdot 10^{-2}$ g EPS/cm³ of soil. The SWRC were obtained for a large range
302 of suctions (between 0 and 5000 cm). Results showed that the more biomass and lower
303 suctions the larger the soil water retention. At saturation, water contents increased about
304 6% and 24% for the respective fractions, attributed to the swelling forces in EPS.

305 The second data set employed [Rubol *et al.*, 2014] considered a natural and heteroge-
306 neous soil affected by a real bioclogging process. After 12 weeks of continuous infiltration
307 of synthetic water a complex microbial colony proliferated. Specialization of bacteria to
308 the nutrient availability made possible the occurrence of microbial activity in all tank
309 depths [see Freixa *et al.*, 2016, for details]. The weighted (spatially-averaged) amount of
310 biofilm compounds at days 3 and 83 dictated the initial and final biological stages. Using
311 the soil density and a mass of a bacterium of $9.3 \cdot 10^{-13}$ g [from Roane *et al.*, 2009], the
312 grams of bacteria per cm³ of soil were estimated to increase from $5.501 \cdot 10^{-5}$ to $1.574 \cdot 10^{-3}$
313 throughout the experiment. Similarly, the content of EPS was $8.621 \cdot 10^{-5}$ and $1.03 \cdot 10^{-4}$
314 grams of EPS per cm³ of soil (by simple analogy, we used the physical characteristics of
315 xanthan). Therefore, the total mass of biofilm (sum of bacteria and EPS) underwent more

316 than a ten-fold increase. For convenience, given that the initial M_{bio} was very small, we
317 considered the relative increase instead of the absolute numbers. Thus the total biofilm
318 proliferation was $1.536 \cdot 10^{-3}$ g biofilm/cm³, equivalent to a biomass fraction in soil of
319 about 0.1%. A global rise of the water held was also noticed. The weighted mean of the
320 water content at saturation increased by 6%. Design limitations restricted the induced
321 suctions between 100 and -100 cm.

322 These two experiments revealed significant displacements of the SWRC towards higher
323 saturations (Figure 6). The hydraulic parameters of these soils are summarized in Table 1.
324 In general terms, θ_s and θ_r increase with the amount of biomass, and α does the opposite.
325 However, even though n is closely related to the pore-size distribution, a direct pattern
326 was not observed.

327 Figure 6 compares the aforementioned experiments with the BCC-PSSICO model and
328 two other models. First is the macroscopic model of *Rockhold et al.* [2002], that does
329 not represent the actual distribution and morphology of the biofilm, and further neglects
330 shrinking and swelling capacity. Consequently, results show a poor fit with this model,
331 which is seen to require a substantial amount of biomass to obtain noticeable changes
332 in the SWRC. Even then, fit is still not good because moisture at low suctions decrease
333 proportionally to the amount of microbial phase (slightly observed at the bottom of the
334 Figure 6, left). Second, the linear superposition model [*Rosenzweig et al.*, 2012] does
335 take into account the capacity of the biofilm to retain variable amounts of water. This
336 model results from direct superposition of the original soil and the xanthan characteristics.
337 Surprisingly, despite this model is not process-based, a relatively good match is observed in
338 the Rosenzweig's soil data. This denotes that the macroscopic water retention properties

339 of biofilms itself may reproduce changes under certain conditions. However, the same
340 model cannot reproduce the event observed in Rubol's soil.

341 The use of mechanistically-based models allows us to better understanding processes and
342 obtain good approaches in a wider range of situations. In this line, it is worth mentioning
343 the works of *Rosenzweig et al.* [2009, 2014]. The study of different scenarios revealed the
344 importance of biofilm distribution. Similar that in *Rockhold et al.* [2002], results obtained
345 are conditioned by the presence of solids in biofilms, which was neglected in our model.
346 This effect seems to be significant at large biofilm saturations, albeit it may be masked by
347 other processes such as the change in soil porosity. Results from scenarios in *Rosenzweig*
348 *et al.* [2009] lay far from data points because the authors neglected the effect of suction on
349 biofilms (results not shown). Thus, despite it is beyond the scope of this study, it would
350 be interesting to extend the model by reformulating (17) according to other pore-scale
351 distribution patterns.

352 It is worth noting that the BCC-PSSICO model provides a good fit to the Rosenzweig's
353 soil data even when the simplest $N = 1$ model is considered. Data is also well reproduced
354 by the linear superposition model for a wide range of suctions. This indicates that when
355 no spatial competition between water phases occurs, the SWRC may be effectively repro-
356 duced by using macroscopic models. To obtain the best fit between to the observations,
357 we used inverse modeling calibration based on the Levenberg-Marquardt algorithm for
358 nonlinear regression. Through calibration, our model is able to fit the changes even in
359 the heterogeneous soil. The voids and channels observed in Figure 1 support the large
360 N values estimated. However, differences between the two data sets are strikingly large.
361 We hypothesize that the mechanical mixing employed in *Rosenzweig et al.* [2012] may

362 not reproduce the proper architecture of a biofilm, but this hypothesis still needs further
363 confirmation in additional studies. In general terms, N is linked to the actual and histori-
364 cal environmental conditions surrounding biofilm, such as the flow rate and the substrate
365 conditions [supported by *Kim et al.*, 2010; *Thullner*, 2010]. Such a intricate morphologies
366 are a beneficial strategy because they reduce the shear stresses (flow) while increasing the
367 diffusion of nutrients (exchange surface). This is quite a clear evidence that models should
368 incorporate complex geometries instead of a simple one consisting of a layer attached to
369 the tube walls.

5. Impact of Bioclogging on the Soil Hydraulic Properties

5.1. Impact of Bioclogging on the SWRC

370 The sensitivity of the SWRC to the parameters N and M_{bio} is illustrated in Figures
371 7 and 8. To simplify, we took the soil hydraulic parameters from the biofilm-free soil
372 from *Rubol et al.* [2014] and neglected the effect of bacteria (only EPS was considered).
373 Despite different combinations of the parameters may produce similar SWRC, substantial
374 differences are observed in the distribution of water in pore-matrix or in biofilms. On the
375 one hand, it should be pointed out that the choice of N does not affect the biofilm volume
376 but its structure, giving rise to changes in the pore-size distribution. The density of small
377 tubes increases with N . Thus, more pores are filled with water at each given suction. Such
378 a mechanism can be so strong that may even convert the holding capacity of a sandy soil
379 into a clay-like soil, regardless of the quantity of biomass. This way, even small amounts of
380 biofilm may fully modify water partitioning leading to significant changes in soil properties.
381 On the other hand, M_{bio} leads to changes in the moisture content based on the amount of
382 water retained in both the biofilm bodies and in the modified pore-matrix. The presence of

383 biofilm is at the expense of the free-space available. Such a phenomenon can be observed
 384 specially at low suctions, where $\theta_{w,pm}$ becomes very small or even disappears. Therefore,
 385 the amount of water held by the biofilms (directly or indirectly) is determined by the
 386 microbial mass, its architecture, and its capacity to shrink/swell.

5.2. Impact of Bioclogging on Permeability

387 Figure 9 shows the relative permeability of a biofilm-free and five bio-amended soils. In
 388 principle, permeability should decrease when suction rises due to the shrinkage of the area
 389 available for water flow. However, dealing with complex biofilms requires further attention
 390 because the accumulation of biomass reshapes the pore-matrix in such a way that the
 391 overall flow capacity is affected. In general, the hydraulic conductivity of soils drops when
 392 clogging occurs because flow paths become blocked to some extent. Such a phenomenon
 393 admits further clarification due to the utilization of physical-based parameters in the
 394 model. On the one hand, the permeability of soils tends to decrease as the structural
 395 complexity of biofilm rises, related to the significance of the tube radius in (24). As a
 396 result, the presence of even small amounts of biofilm may cause a significant impact on
 397 k_r (note the drop when $N \gg 1$). On the other hand, the specific contribution of biofilm
 398 bodies to flow depends mostly on how its conductance is defined in (6) and (7).

399 In order to highlight the role of N and M_{bio} , μ_{bio} is first defined as constant, ignoring the
 400 effect of swelling in viscosity (Figure 9, top). The definition of a fully-permeable ($\lambda_\mu = 1$),
 401 semi-permeable or impermeable biofilm ($\lambda_\mu = \infty$) brings about significant changes in the
 402 overall permeability of the medium. On the other hand, when biofilm behaves like an
 403 impermeable body, clogging most likely occurs. In general, the larger the value of N
 404 and M_{bio} the more significant the permeability drop. However, it is worth mentioning

405 the opposite effect occurring for complex biofilm architectures (expressed by large N).
406 Even though the contribution of the biofilm bodies is zero, the simple increase in open-
407 pore water at high suctions may lead to a permeability rise. On the other hand, highly
408 conductive biofilms induce a clear increase of the flow capacity of soils for a wide range of
409 suctions. The effect of suction changes in λ_μ presents little but significant characteristics
410 that make the difference (Figure 9, bottom). k_r is a result of the balance between the
411 expressions for the biofilm volume changes in (4) and its permeability in (7).

412 A comparison of results to experimental data can hardly provide conclusive informa-
413 tion because clogging effects reported in the literature poorly correlate with the amount
414 of biomass. On the one hand, experimental studies reported hydraulic conductivity re-
415 ductions ranging from one [e.g., *Rubol et al.*, 2014; *Volk et al.*, 2016; *Zhong and Wu*, 2013]
416 to a few orders of magnitude [e.g., *Engesgaard et al.*, 2006; *Or et al.*, 2007b; *Taylor and*
417 *Jaffé*, 1990; *Vandevivere and Baveye*, 1992b]. Although relevant data under unsaturated
418 conditions is scarce, the recent work of *Volk et al.* [2016] provided detailed direct mea-
419 surements in which permeability was reduced by a factor of four. On the other hand, the
420 models of permeability in unsaturated soils are so far quite limited. Even though a few
421 approaches constituted a great advance in modeling [e.g., *Mostafa and Van Geel*, 2007;
422 *Rosenzweig et al.*, 2009] we believe that the capacity of bio-amended soils to let water
423 through is not properly treated. In this line, our model does include a complex (and
424 realistic) representation of biofilm that is capable of predicting permeability reductions
425 of distinct orders of magnitude, similar to the ones found in the literature. Results show
426 that the permeability of bio-amended soils is a function of the biofilm conductance and of
427 the distribution of phases (open-pore water and biofilm) in the tube cross-sections, with

428 a certain emphasis on the biofilm architecture (N). The more complex characterization of
429 biofilms is at the expense of the pore space definition. Despite of that the pore intercon-
430 nectivity is required to reflect the complexity of the multidimensional flow in real porous
431 media, a simple analysis using our model already provides a rough estimation of the rela-
432 tive permeability at some intermediate scale. The number of parameters studied and the
433 need to define the flow through pore interconnections hamper determining whether such
434 a simplification over- or underpredicts the real impact on soils. The lack of knowledge
435 on this point together with the uncertainties illustrated in Figure 9 underline the need of
436 further research.

437 Despite the importance of the transport of nutrients for biofilm growth, and the mo-
438 bilization of contaminants in many fields, we consider it to be out of the scope of this
439 paper. Here, we just state that the geometries discussed above also entail consequences
440 in transport, as the interfaces through which mass is exchanged are redefined, modifying
441 the exposure, nutrients availability, and removal rates.

6. Conclusions

442 The growth of biofilm in soils exerts a strong influence on hydraulic parameters, modi-
443 fying the shape of the water retention curve and the relative permeability. We present a
444 model that aims at improving our understanding of such a phenomenon. Our approach
445 consists in modeling the local characteristics of soil as an ensemble of capillary tubes of
446 different diameters. This simple (and widely used in biofilm-free soils) methodology is ex-
447 tended by the incorporation of a biofilm composed of bacterial cells and EPS. Three main
448 points are considered: i) biofilm alone is capable of holding large amounts of water and
449 has particular hydraulic properties; ii) microbial phase undergoes changes in volume; and

450 iii) biofilm is not a convex surface but a channeled complex geometry (which allows us to
451 redefine the concept of tubes that are colonized by a biofilm with complex geometries). On
452 the basis of these points, the new properties of the bio-colonized soil are derived yielding
453 a set of analytical equations that account for the spatial competition between open-pore
454 water and biofilm at pore-scale. First, the incorporation of channeled biofilm bodies that
455 shrink/swell enables us to obtain a new pore-size distribution from which the soil-water
456 retention curve is derived. Subsequently, the geometrical distribution of a permeable
457 biofilm in tubes provides an approach to relative permeability. Such a flexible framework
458 can incorporate with no effort other type of hypotheses regarding biofilm characteristics
459 and distribution. Assumptions based on the tube theory vastly underestimate pore singu-
460 larities, simplifying its geometry and interconnections and possibly underpredicting water
461 content distribution and flow rates. The current model can be understood as a tool to
462 isolate and better study the local impact of biofilms on the hydraulic properties.

463 The new expression for the SWRC is evaluated by the data of three bio-amended soils.
464 The model can properly reproduce the displacement of the SWRC towards higher satura-
465 tions. Moreover, a sensitivity analysis on both the SWRC and the relative permeability
466 functions is performed in order to understand the role of the parameters presented. From
467 it, we could explain how even small amounts of biofilm may fully reshape the pore network
468 leading to significant changes in hydraulic properties. Results indicate that the morphol-
469 ogy, the spatial distribution of biomass and the EPS swelling and shrinking characteristics
470 are key factors controlling the properties of bio-amended soils. The number of hypothe-
471 ses included in the model enhances the need for a sound analysis of these properties of

472 biofilms, as they play a major role in the overall soil behavior and therefore they should
473 be included somehow in biofilm modeling.

474 **Acknowledgments.** The research leading to these results has received funding from
475 the European Union FP7 under grant agreement no 619120 (Demonstrating Man-
476 aged Aquifer Recharge as a Solution to Water Scarcity and Drought MARSOL), and
477 PCOFUND-GA-2008-226070. Additional support was provided by the Spanish Ministry
478 of Economy and Competitiveness (project SCARCE, ref. CSD2009-00065), and the Min-
479 istry of Science and Innovation (project FEAR, ref. CGL2012-38120; and the research
480 fellowship FPI BES-2013-063419). XS acknowledges support from the ICREA Academia
481 Program. We would like to thank three anonymous reviewers and the associate editor
482 for their constructive comments. We also thank George von Knorring for reviewing the
483 English of an early version of the manuscript. Data can be requested by contacting the
484 corresponding author.

References

- 485 Abdel-Waly, A. (2013), Laboratory Study On Activating Indigenous Microorganisms
486 to Enhance Oil Recovery, *Journal of Canadian Petroleum Technology*, 38(02), doi:
487 10.2118/99-02-05.
- 488 Alaoui, A., J. Lipiec, and H. H. Gerke (2011), A review of the changes in the soil pore
489 system due to soil deformation: A hydrodynamic perspective, *Soil and Tillage Research*,
490 115-116, 1–15, doi:10.1016/j.still.2011.06.002.
- 491 Baveye, P., P. Vandevivere, B. L. Hoyle, P. C. DeLeo, and D. S. de Lozada (1998),
492 Environmental Impact and Mechanisms of the Biological Clogging of Saturated Soils and

- 493 Aquifer Materials, *Critical Reviews in Environmental Science and Technology*, 28(2),
494 123–191, doi:10.1080/10643389891254197.
- 495 Beckett, C., and C. Augarde (2013), Prediction of soil water retention properties using
496 pore-size distribution and porosity, *Canadian Geotechnical Journal*, 450(April), 435–
497 450, doi:10.1139/cgj-2012-0320.
- 498 Billings, N., A. Birjiniuk, T. S. Samad, P. S. Doyle, and K. Ribbeck (2015), Material
499 properties of biofilms a review of methods for understanding permeability and mechanics,
500 *Reports on Progress in Physics*, 78(3), 036,601, doi:10.1088/0034-4885/78/3/036601.
- 501 Bozorg, A., I. D. Gates, and A. Sen (2015), Using bacterial bioluminescence to evaluate
502 the impact of biofilm on porous media hydraulic properties, *Journal of Microbiological*
503 *Methods*, 109, 84–92, doi:10.1016/j.mimet.2014.11.015.
- 504 Brooks, R. H., and A. T. Corey (1964), Hydraulic properties of porous media, *Hydrology*
505 *papers Colorado State University*, 3.
- 506 Bundt, M., F. Widmer, M. Pesaro, J. Zeyer, and P. Blaser (2001), Preferential flow paths:
507 Biological 'hot spots' in soils, *Soil Biology and Biochemistry*, 33(6), 729–738.
- 508 Burdine, N. (1953), Relative Permeability Calculations From Pore Size Distribution Data,
509 doi:10.2118/225-G.
- 510 Carsel, R., and R. Parrish (1988), Developing joint probability distributions of soil water
511 retention characteristics, *Water Resources Research*, 24(5), 755–769.
- 512 Castegnier, F., N. Ross, R. P. Chapuis, L. Deschênes, and R. Samson (2006), Long-term
513 persistence of a nutrient-starved biofilm in a limestone fracture., *Water research*, 40(5),
514 925–34, doi:10.1016/j.watres.2005.12.038.

- 515 Chenu, C. (1993), Clay-or sand-polysaccharide associations as models for the interface
516 between micro-organisms and soil: water related properties and microstructure, *Geo-*
517 *derma*, 56(1-4), 143–156.
- 518 Christensen, T. H., P. L. Bjerg, S. A. Banwart, R. Jakobsen, G. Heron, and H.-J. Albrecht-
519 sen (2000), Characterization of redox conditions in groundwater contaminant plumes,
520 *Journal of Contaminant Hydrology*, 45(3-4), 165–241.
- 521 Clement, T., B. Hooker, and R. Skeen (1996), Macroscopic models for predicting changes
522 in saturated porous media properties caused by microbial growth, *Groundwater*, 34(5),
523 934–942.
- 524 Cooke, R., and I. D. Kuntz (1974), The properties of water in biological
525 systems, *Annual Review of Biophysics and Bioengineering*, 3, 95–126, doi:
526 10.1146/annurev.bb.03.060174.000523.
- 527 Cunningham, A., R. Gerlach, L. Spangler, and A. Mitchell (2009), Microbially enhanced
528 geologic containment of sequestered supercritical CO₂, *Energy Procedia*, 1(1), 3245–
529 3252, doi:10.1016/j.egypro.2009.02.109.
- 530 Cunningham, A. B., w. G. Characklis, F. Abedeen, and D. Crawford (1991), Influence
531 of biofilm accumulation on porous media hydrodynamics, *Environmental Science and*
532 *Technology*, 25 (7), 1305–1311.
- 533 Davit, Y., H. Byrne, J. Osborne, J. Pitt-Francis, D. Gavaghan, and M. Quintard (2013),
534 Hydrodynamic dispersion within porous biofilms, *Physical Review E - Statistical, Non-*
535 *linear, and Soft Matter Physics*, 87(1), 24–29, doi:10.1103/PhysRevE.87.012718.
- 536 De Beer, D., and A. Schramm (1999), Micro-environments and mass transfer phenomena
537 in biofilms studied with microsensors, in *Water Science and Technology*, vol. 39, pp.

- 538 173–178, doi:10.1016/S0273-1223(99)00165-1.
- 539 de Gennes, P.-G. (1979), *Scaling Concepts in Polymer Physics*, Cornell University Press.
- 540 De Muynck, W., N. De Belie, and W. Verstraete (2010), Microbial carbonate precip-
541 itation in construction materials: A review, *Ecological Engineering*, *36*(2), 118–136,
542 doi:10.1016/j.ecoleng.2009.02.006.
- 543 DeJong, J., K. Soga, and E. Kavazanjian (2013), Biogeochemical processes and geotechni-
544 cal applications: progress, opportunities and challenges, *Géotechnique*, *63*(4), 287–301.
- 545 Donlan, R. M. (2002), Biofilms: Microbial life on surfaces, doi:10.3201/eid0809.020063.
- 546 Dupin, H. J., P. K. Kitanidis, and P. L. McCarty (2001), Pore-scale modeling of biological
547 clogging due to aggregate expansion: A material mechanics approach, *Water Resources*
548 *Research*, *37*(12), 2965–2979, doi:10.1029/2001WR000306.
- 549 Ehrlich, H. L. (1999), Microbes as Geologic Agents: Their Role in Mineral Formation,
550 *Geomicrobiology Journal*, *16*(2), 135–153, doi:10.1080/014904599270659.
- 551 Engesgaard, P., D. Seifert, and P. Herrera (2006), Bioclogging in porous media: tracer
552 studies, in *Riverbank Filtration Hydrology*, vol. 60, pp. 93–118, Springer Netherlands.
- 553 Ezeuko, C., A. Sen, A. Griogoryan, and G. I.D. (2011), Pore-network modeling of biofilm
554 evolution in porous media, *Biotechnology and Bioengineering*, *108*(10), 2413–2423, doi:
555 10.1002/bit.23183.
- 556 Fenchel, T. (2002), Microbial behavior in a heterogeneous world, *Science*, *296*(5570),
557 1068–1071, doi:10.1126/science.1070118.
- 558 Flemming, H.-C., and J. Wingender (2010), The biofilm matrix, *Nature reviews. Micro-*
559 *biology*, *8*(9), 623–33, doi:10.1038/nrmicro2415.

- 560 Freixa, A., S. Rubol, A. Carles-Brangarí, D. Fernández-García, A. Butturini, X. Sanchez-
561 Vila, and A. M. Romani (2016), The effects of sediment depth and oxygen concentration
562 on the use of organic matter : An experimental study using an in fi ltration sediment
563 tank, *Science of the Total Environment*, *540*, 20–31, doi:10.1016/j.scitotenv.2015.04.007.
- 564 Hand, V. L., J. R. Lloyd, D. J. Vaughan, M. J. Wilkins, and S. Boulton (2008), Experimental
565 studies of the influence of grain size, oxygen availability and organic carbon availability
566 on bioclogging in porous media, *Environmental Science & Technology*, *42*(5), 1485–
567 1491.
- 568 Kennedy, P. L., and P. J. Van Geel (2001), Impact of density on the hydraulics of peat
569 filters, *Canadian Geotechnical Journal*, *38*, 1213–1219, doi:10.1139/t01-047.
- 570 Kim, J., H. Choi, and Y. Pachepsky (2010), Biofilm morphology as related to the porous
571 media clogging, *Water Research*, *44*(4), 1193–1201, doi:10.1016/j.watres.2009.05.049.
- 572 Laspidou, C. S., and B. E. Rittmann (2004), Modeling the development of biofilm density
573 including active bacteria, inert biomass, and extracellular polymeric substances, *Water*
574 *Research*, *38*(14-15), 3349–3361, doi:10.1016/j.watres.2004.04.037.
- 575 Lawrence, J. R., D. R. Korber, B. D. Hoyle, J. W. Costerton, and D. E. Caldwell (1991),
576 Optical sectioning of microbial biofilms, *Journal of Bacteriology*, *173*, 6558–6567.
- 577 Likos, W., and R. Jaafar (2013), Pore-scale model for water retention and fluid partition-
578 ing of partially saturated granular soil, *Journal of Geotechnical and Geoenvironmental*
579 *Engineering*, *139*(5), 724–737, doi:10.1061/(ASCE)GT.1943-5606.0000811.
- 580 Mauclair, L., A. Schürmann, and F. Mermillod-Blondin (2006), Influence of hydraulic
581 conductivity on communities of microorganisms and invertebrates in porous media: a
582 case study in drinking water slow sand filters, *Aquatic Sciences*, *68*(1), 100–108, doi:

583 10.1007/s00027-005-0811-4.

584 Mitchell, J. K., and K. Soga (2005), Soil Composition and Engineering Properties, in
585 *Fundamentals of Soil Behavior*, pp. 83–108, CBS Publishers & Distributors Pvt. Ltd.

586 Morris, R. H., M. I. Newton, P. R. Knowles, M. Bencsik, P. A. Davies, P. Griffin, and
587 G. McHale (2011), Analysis of clogging in constructed wetlands using magnetic reso-
588 nance, *The Analyst*, 136, 2283–2286, doi:10.1039/c0an00986e.

589 Mostafa, M., and P. Van Geel (2012), Validation of a Relative Permeability Model for Bio-
590 clogging in Unsaturated Soils, *Vadose Zone Journal*, 11(1), doi:10.2136/vzj2011.0044.

591 Mostafa, M., and P. J. Van Geel (2007), Conceptual Models and Simulations for
592 Biological Clogging in Unsaturated Soils, *Vadose Zone Journal*, 6(1), 175, doi:
593 10.2136/vzj2006.0033.

594 Mualem, Y. (1976), A new model for predicting the hydraulic conductivity of unsaturated
595 porous media, *Water Resources Research*, 12(3).

596 Or, D., B. Smets, and J. Wraith (2007a), Physical constraints affecting bacterial habitats
597 and activity in unsaturated porous mediaa review, *Advances in Water Resources*, 30(6-
598 7), 1505–1527.

599 Or, D., S. Phutane, and A. Dechesne (2007b), Extracellular polymeric substances affecting
600 pore-scale hydrologic conditions for bacterial activity in unsaturated soils, *Vadose Zone*
601 *Journal*, 6(2), 298–305, doi:10.2136/vzj2006.0080.

602 Pedretti, D., M. Barahona-Palomo, B. Diogo, D. Fernández-García, X. Sanchez-Vila,
603 and D. M. Tartakovsky (2012), Probabilistic analysis of maintenance and operation
604 of artificial recharge ponds, *Advances in Water ...*, 36(April 2011), 23–35, doi:
605 10.1016/j.advwatres.2011.07.008.

- 606 Peña-Cabriaes, J. J., and M. Alexander (1979), Survival of Rhizobium in Soils
607 Undergoing Drying, *Soil Science Society of America Journal*, 43(5), 962, doi:
608 10.2136/sssaj1979.03615995004300050030x.
- 609 Picioreanu, C., J. Xavier, and M. van Loosdrecht (2004), Advances in mathematical
610 modeling of biofilm structure, *Biofilms*, 1(4), 337–349, doi:10.1017/S1479050505001572.
- 611 Pintelon, T. R. R., C. Picioreanu, M. C. M. van Loosdrecht, and M. L. Johns (2012),
612 The effect of biofilm permeability on bioclogging of porous media, *Biotechnology and*
613 *Bioengineering*, 109(4), 1031–1042, doi:10.1002/bit.24381.
- 614 Qin, C.-Z., and S. M. Hassanizadeh (2015), Pore-Network Modeling of Solute Transport
615 and Biofilm Growth in Porous Media, *Transport in Porous Media*, 110(3), 345–367,
616 doi:10.1007/s11242-015-0546-1.
- 617 Rebata-Landa, V., and J. C. Santamarina (2012), Mechanical Effects of Biogenic Nitrogen
618 Gas Bubbles in Soils, doi:10.1061/(ASCE)GT.1943-5606.0000571.
- 619 Rittmann, B. (1993), The significance of biofilms in porous media, *Water Resources Re-*
620 *search*, 29(7), 2195–2202.
- 621 Roane, T. M., K. A. Reynolds, R. M. Maier, and I. L. Pepper (2009), *Environmental*
622 *Microbiology*, 9–36 pp., Elsevier, doi:10.1016/B978-0-12-370519-8.00002-X.
- 623 Rockhold, M., R. Yarwood, M. Niemet, P. Bottomley, and J. Selker (2002), Considerations
624 for modeling bacterial-induced changes in hydraulic properties of variably saturated
625 porous media, *Advances in Water Resources*, 25(5), 477–495.
- 626 Rodríguez-Escales, P., A. Folch, B. M. van Breukelen, G. Vidal-Gavilan, and X. Sanchez-
627 Vila (2016), Modeling long term Enhanced in situ Bionitrification and induced hetero-
628 geneity in column experiments under different feeding strategies, *Journal of Hydrology*,

- 629 538, 127–137, doi:10.1016/j.jhydrol.2016.04.012.
- 630 Rosenzweig, R., U. Shavit, and A. Furman (2009), The influence of biofilm spatial distri-
631 bution scenarios on hydraulic conductivity of unsaturated soils, *Vadose Zone Journal*,
632 8(4), 1080, doi:10.2136/vzj2009.0017.
- 633 Rosenzweig, R., U. Shavit, and A. Furman (2012), Water retention curves of biofilm-
634 affected soils using xanthan as an analogue, *Soil Science Society of America Journal*,
635 76(1), 61–69, doi:10.2136/sssaj.
- 636 Rosenzweig, R., A. Furman, and U. Shavit (2013), A channel network model as a frame-
637 work for characterizing variably saturated flow in biofilm-affected soils, *Vadose Zone*
638 *Journal*, 12(2), doi:10.2136/vzj2012.0079.
- 639 Rosenzweig, R., A. Furman, C. Dosoretz, and U. Shavit (2014), Modeling biofilm dynamics
640 and hydraulic properties in variably saturated soils using a channel network model,
641 *Water Resources Research*, 50, 5678–5697, doi:10.1002/2013WR015211.
- 642 Ross, N., R. Villemur, L. Deschênes, and R. Samson (2001), Clogging of a limestone
643 fracture by stimulating groundwater microbes, *Water Research*, 35, 2029–2037, doi:
644 10.1016/S0043-1354(00)00476-0.
- 645 Rubol, S., A. Freixa, A. Carles-Brangarí, D. Fernàndez-Garcia, A. M. Romaní, and
646 X. Sanchez-Vila (2014), Connecting bacterial colonization to physical and biochemi-
647 cal changes in a sand box infiltration experiment, *Journal of Hydrology*, 517, 317–327,
648 doi:10.1016/j.jhydrol.2014.05.041.
- 649 Samsó, R., and J. García (2014), The Cartridge Theory: a description of the func-
650 tioning of horizontal subsurface flow constructed wetlands for wastewater treatment,
651 based on modelling results., *The Science of the Total Environment*, 473-474, 651–8,

- 652 doi:10.1016/j.scitotenv.2013.12.070.
- 653 Seki, K., T. Miyazaki, and M. Nakano (1998), Effects of microorganisms on hydraulic
654 conductivity decrease in infiltration, *European Journal of Soil Science*, *49*(2), 231–236.
- 655 Selker, J. S., J. T. McCord, and C. K. Keller (1999), *Vadose Zone Processes*, 352 pp.,
656 CRC Press.
- 657 Soleimani, S., P. J. Van Geel, O. B. Isgor, and M. B. Mostafa (2009), Modeling of biological
658 clogging in unsaturated porous media, *Journal of Contaminant Hydrology*, *106*(1-2),
659 39–50, doi:10.1016/j.jconhyd.2008.12.007.
- 660 Stewart, P. S. (2012), Mini-review: convection around biofilms., *Biofouling*, *28*(2), 187–98,
661 doi:10.1080/08927014.2012.662641.
- 662 Stoodley, P., D. DeBeer, and Z. Lewandowski (1994), Liquid flow in biofilm systems,
663 *Applied and Environmental Microbiology*, *60*(8), 2711–2716.
- 664 Stoodley, P., K. Sauer, D. G. Davies, and J. W. Costerton (2002), Biofilms as com-
665 plex differentiated communities., *Annual review of microbiology*, *56*, 187–209, doi:
666 10.1146/annurev.micro.56.012302.160705.
- 667 Tamaru, Y., Y. Takani, T. Yoshida, and T. Sakamoto (2005), Crucial role of extracellular
668 polysaccharides in desiccation and freezing tolerance in the terrestrial cyanobacterium
669 *Nostoc commune*, *Applied and Environmental Microbiology*, *71*(11), 7327–7333, doi:
670 10.1128/AEM.71.11.7327-7333.2005.
- 671 Taylor, S. W., and P. R. Jaffé (1990), Biofilm growth and the related changes in the
672 physical properties of a porous medium: 1. Experimental investigation, *Water Resources*
673 *Research*, *26*(9), 2153–2159, doi:10.1029/WR026i009p02153.

- 674 Taylor, S. W., P. Milly, and P. R. Jaffe (1990), Biofilm Growth and the Related Changes in
675 the Physical Properties of a Porous Medium. 2. Permeability, *Water Resources Research*
676 *WRERAQ*, *26*(9).
- 677 Thullner, M. (2010), Comparison of bioclogging effects in saturated porous media within
678 one- and two-dimensional flow systems, *Ecological Engineering*, *36*(2), 176–196, doi:
679 10.1016/j.ecoleng.2008.12.037.
- 680 Thullner, M., and P. Baveye (2008), Computational pore network modeling of the influence
681 of biofilm permeability on bioclogging in porous media, *Biotechnology and Bioengineer-*
682 *ing*, *99*(6), 1337–1351, doi:10.1002/bit.21708.
- 683 Van Cuyk, S., R. Siegrist, A. Logan, S. Masson, E. Fischer, and L. Figueroa (2001),
684 Hydraulic and purification behaviors and their interactions during wastewater treat-
685 ment in soil infiltration systems, *Water Research*, *35*, 953–964, doi:10.1016/S0043-
686 1354(00)00349-3.
- 687 van Genuchten, M. T. (1980), A closed-form equation for predicting the hydraulic con-
688 ductivity of unsaturated soils, *Soil science society of America Journal*, *44*(5).
- 689 Vandevivere, P., and P. Baveye (1992a), Saturated Hydraulic Conductivity Reduction
690 Caused by Aerobic Bacteria in Sand Columns, *Soil Science Society of America Journal*,
691 *56*, 1–13, doi:10.2136/sssaj1992.03615995005600010001x.
- 692 Vandevivere, P., and P. Baveye (1992b), Effect of bacterial extracellular polymers on the
693 saturated hydraulic conductivity of sand columns, *Applied and Environmental Micro-*
694 *biology*, *58*(5), 1690–1698.
- 695 Vandevivere, P., P. Baveye, D. Sanchez de Lozaa, and P. DeLeo (1995), Microbial clogging
696 of saturated soils and aquifer materials: Evaluation of mathematical models, *Water*

- 697 *Resources Research*, 31(9), 2173–2180.
- 698 Volk, E., S. C. Iden, A. Furman, W. Durner, and R. Rosenzweig (2016), Biofilm effect
699 on soil hydraulic properties: Experimental investigation using soil-grown real biofilm,
700 *Water Resources Research*, pp. 1–20, doi:10.1002/2016WR018866.
- 701 Wagner, M., D. Taherzadeh, C. Haisch, and H. Horn (2010), Investigation of the mesoscale
702 structure and volumetric features of biofilms using optical coherence tomography.,
703 *Biotechnology and bioengineering*, 107(5), 844–53, doi:10.1002/bit.22864.
- 704 Wilking, J. N., T. E. Angelini, A. Seminara, M. P. Brenner, and D. a. Weitz (2011),
705 Biofilms as complex fluids, *MRS Bulletin*, 36(05), 385–391, doi:10.1557/mrs.2011.71.
- 706 Yarwood, R., M. Rockhold, M. Niemet, J. Selker, and P. Bottomley (2006), Impact of
707 microbial growth on water flow and solute transport in unsaturated porous media,
708 *Water Resources Research*, 42(10), doi:10.1029/2005WR004550.
- 709 Young, I. M., and J. W. Crawford (2004), Interactions and self-organization in the soil-
710 microbe complex., *Science*, 304, 1634–1637, doi:10.1126/science.1097394.
- 711 Zhang, T. C., Y. Fu, P. L. Bishop, M. Kupferle, S. FitzGerald, H. H. Jiang, and C. Harmer
712 (1995), Transport and biodegradation of toxic organics in biofilms, *Journal of Hazardous*
713 *Materials*, 41, 267–285, doi:10.1016/0304-3894(94)00118-Z.
- 714 Zhong, X., and Y. Wu (2013), Bioclogging in porous media under continuous-flow condi-
715 tion, *Environmental Earth Sciences*, 68(8), 2417–2425, doi:10.1007/s12665-012-1926-2.

Figure 1. Images of biofilms showing heterogeneous structure. Left: mature biofilm forming voids and channels between two soil grains [modified from *Hand et al.*, 2008]. Right: Stained EPS and bacteria developed on a steel surface [modified from *Donlan*, 2002].

Figure 2. Estimate of λ_μ due to changes in the water content of the biofilm caused by swelling/shrinking processes, based on (7).

Figure 3. Solid (mineral), biofilm, water and air phases present in a bio-amended soil under variably suction stress. Left: distribution of the different phases within the total volume. Right: cross-sections of the capillary tubes, displaying the spatial distribution of air, open-pore water and water in biofilm. For each suction value, only the tubes (of the newly defined pore-matrix) smaller than R remain fully saturated while the others have the specific amount of water relative to the volume of biofilm they content.

Figure 4. Sketch showing how N modifies the pore-size distribution of the porous medium. This has a direct impact on the volumetric water content. The top scenario depicts the behavior of a biofilm-free soil whereas the others reproduce the changes in the distribution of phases with N . $\theta_{w,bio}$ and ψ remain constant in all cases.

Figure 5. Sketch of the geometrical distribution of biofilm and its impact upon flow. The permeability approach requires a slight modification of the geometry. Symmetry around the central axis is recovered while the areas of the phases are still conserved. Left: A tube of radius r_0 is redefined as a tube of radius $r + \delta$ for mathematical convenience. Right: a single tube of radius r_0 is transformed into four new pore-matrix tubes ($N = 4$) of radius $r + \delta$. Green areas are microbial phase cross-sections through which water flows. When $r > R$ (left case), despite flow is not allowed through the pore-matrix, the microbial phase does contribute to flow.

Figure 6. Comparison of bioclogging models with experimental data reported by *Rosenzweig et al.* [2012], left figure, and *Rubol et al.* [2014], right figure. The bioclogging models presented include the BCC-PSSICO model, the macroscopic model of *Rockhold et al.* [2002] and the linear superposition model by *Rosenzweig et al.* [2012].

Figure 7. Effect of N on the water holding capacities of the composite medium (left, in black), distinguishing between water in the pore-matrix (middle, in brown) and pure biofilm (right, in green). The mass fraction of EPS is assumed equal to $5 \cdot 10^{-3}$ g EPS/cm³ in order to isolate the effect of N .

Figure 8. Effect of M_{bio} on the volumetric water content for $N = 1$ (top) and $N = 10$ (bottom), distinguishing between water in the pore-matrix (middle, in brown) and pure biofilm (right, in green). The mass of biofilm is expressed in g EPS/cm³.

Figure 9. Effect of different combinations of N , and M_{bio} on the relative permeability for soils. Lines correspond to the biofilm-free soil (red line), and five theoretical bio-amended soils. The mass of biofilm is expressed in g EPS/cm³. Top: the dynamic viscosity of water flowing through biofilms is considered as constant. Regardless of the swelling status, biofilm is defined as impermeable ($\lambda_\mu = \infty$), semi-permeable ($\lambda_\mu = 5$), or fully-permeable ($\lambda_\mu = 1$). Bottom: the parameter accounting for the viscosity changes when biofilm shrinks/swells is evaluated.

Table 1. Parameters of the van Genuchten model and of the amount of biomass. SWRC parameters are obtained from *Rosenzweig et al.* [2012] and using a nonlinear regression on data from *Rubol et al.* [2014]. θ_r in Rubol's soil is evaluated using a linear superposition equation based on the weighted average of the grain-size fractions and hydraulic parameters in *Carsel and Parrish* [1988]. The biological parameters are the estimated values of bacteria, EPS and total biofilm.

<i>Soil</i>	Biomass [%]	ϕ_{ef} [-]	θ_r [-]	n [cm ⁻¹]	α [-]	ρ_s [g/cm ³]	M_{bact} [g/cm ³]	M_{EPS} [g/cm ³]	M_{bio} [g/cm ³]
Rosenzweig	0	0.402	0.026	2.32	0.042	1.56	0	0	0
Rosenzweig	0.25	0.420	0.048	2.11	0.031	-	0	$3.91 \cdot 10^{-3}$	$3.91 \cdot 10^{-3}$
Rosenzweig	1	0.480	0.054	1.89	0.022	-	0	$1.576 \cdot 10^{-2}$	$1.576 \cdot 10^{-2}$
Rubol	0	0.207	0.044	1.63	0.087	1.5	0	0	0
Rubol	0.1	0.222	0.045	2.18	0.029	-	$1.519 \cdot 10^{-3}$	$1.683 \cdot 10^{-5}$	$1.536 \cdot 10^{-3}$

Table 2. Physical properties of water.

σ	$\cos(\beta)$	γ_w	ρ_w	μ_w
$[N/cm]$	$[-]$	$[N/cm^3]$	$[g/cm^3]$	$[sN/cm^2]$
$7.15 \cdot 10^{-4}$	1	$9.789 \cdot 10^{-3}$	0.998	$1.002 \cdot 10^{-7}$

Figure 1.

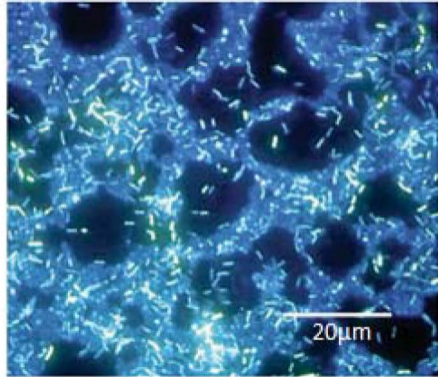
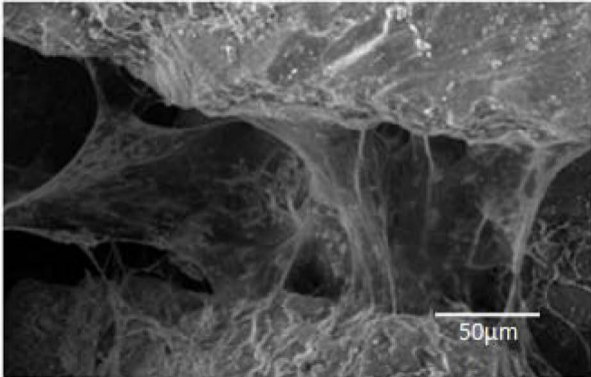


Figure 2.

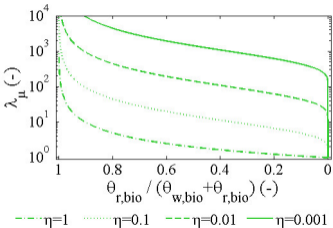


Figure 3.

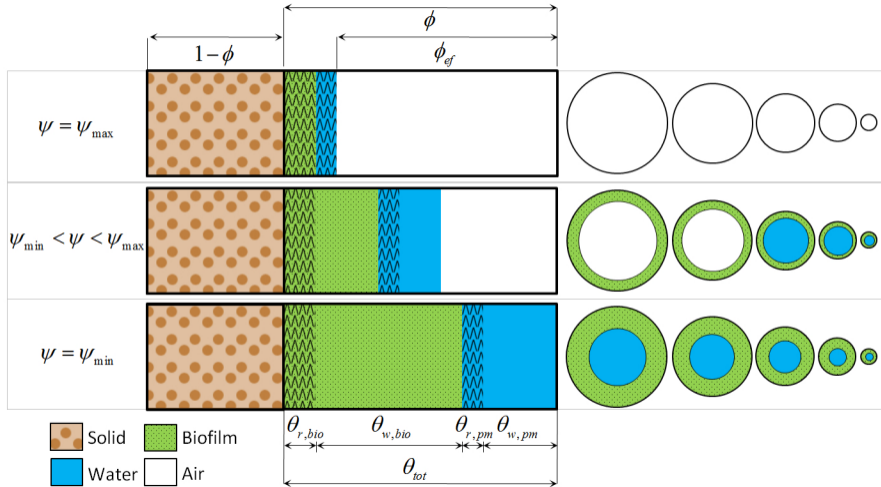
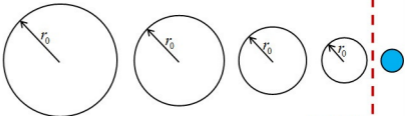


Figure 4.

$$\psi = \Psi$$

$$\theta_{w,bio} = 0$$

$$N \in [1, \infty)$$



$$\psi = \Psi$$

$$\theta_{w,bio} = \Theta$$

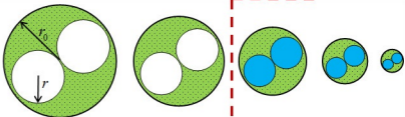
$$N = 1$$



$$\psi = \Psi$$

$$\theta_{w,bio} = \Theta$$

$$N = 2$$



$$\psi = \Psi$$

$$\theta_{w,bio} = \Theta$$

$$N = 4$$

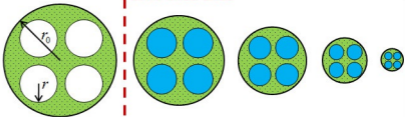
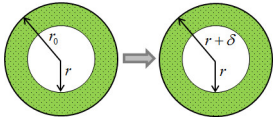

 R/X

Figure 5.

$N = 1$



$N = 4$

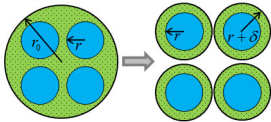
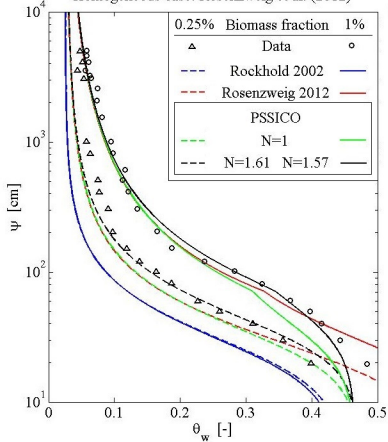


Figure 6.

Homogeneous case: Rosenzweig et al. (2012)



Heterogeneous case: Rubol et al. (2014)

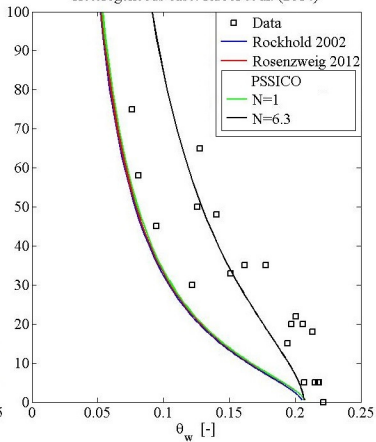


Figure 7.

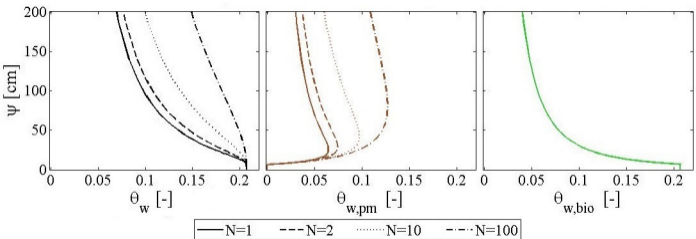


Figure 8.

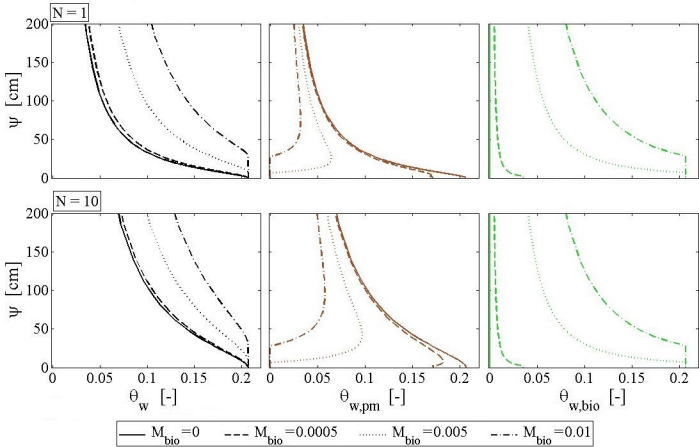


Figure 9.

